Transaction B: Mechanical Engineering
Vol. 17, No. 6, pp. 433–442

SCIENTIA IRANICA

Two-Dimensional Numerical Investigation of a Micro Combustor

A. Irani Rahaghi[1], M.S. Saidi[1,*], M.H. Saidi[1] and M.B. Shafii[1]

Abstract. *In this paper, a two-dimensional numerical approach is used to study the effect of micro combustor height, mass flow rate and external convection heat transfer coefficient on the temperature and species mass fraction profiles. A premixed mixture of H_2-Air with a multi-step chemistry is used. The transient gas phase energy and species conservation equations result in an Advection-Diffusion-Reaction system that leads to two stiff systems of PDEs. In the present work, the computational domain is solved through the Strang splitting method, which is suitable for a nonlinear stiff system of PDEs. A revised boundary condition for the velocity equation is applied and its effect on the flow characteristics is investigated. The results show that both convection heat transfer coefficient and micro combustor height have a significant effect on the combustion and heat transfer rates in the micro scales. Also increasing the convective heat transfer coefficient and decreasing the height and inlet mixture velocity, decreases temperature and active radicals along the micro combustor. In addition, the slip flow and thermal creep boundary conditions in the studied scales have no significant effect on the different parameters, but changes slightly the cross section profiles of the temperature. The 2-D numerical results show that the micro combustion must be treated as two dimensional.*

Keywords: *Micro combustor; Numerical; Combustion; Micro-scale; Two-dimensional.*

INTRODUCTION

Many MEMS-based (Micro Electromechanical Systems) devices, such as micro gas turbines [1], micro reciprocating engines [2], micro thermophotovoltaic systems [3,4], micro fuel cells [5] etc. need a high-density (or a high-specific energy) micro-power supply. Combustion in micro-scales is one of the best ways to provide this power. The demand for this new generation of micro-power source is increasing due to its higher energy density in comparison with conventional batteries. A micro combustor is one of the essential components of micro-power systems, which utilizes the oxidant-fuel mixture (usually air or oxygen as an oxidant and hydrocarbons or hydrogen as a fuel) to release the desired energy. Both thermal and radical quenching mechanisms are important in micro-scale combustion due to increasing the area-to-volume ratio and the significant heat loss from the combustor walls. Therefore, investigation of such components is a key issue in designing a reliable micro-power source. Fernandez-Pello [6] has reviewed some of the technological issues (thermophysical, thermo-fluid and combustion) related to micro combustion and micro power generation devices.

There are different points of view for modeling and simulating the micro-scale combustion systems. Li et al. [7] showed that the reacting flow in the micro scale combustion is 2-D in nature by applying scale analysis. However, 1-D modeling has been used by many researchers to investigate the effect of different parameters on micro combustion. Kaisare and Vlachos [8] noted that the 1-D and 2-D simulation results are quantitatively in good agreement. They studied two mechanisms of thermal quenching: extinction and blowout, and obtained the appropriate reactor length, wall thickness and reactor diameter for self-sustained homogenous combustion in parallel plate channels. They applied one-step homogenous chemistry for two different mixtures (propane-oxygen and methane-oxygen) and used a finite difference scheme to solve the equations numerically. Li et al. [9] developed a 1-D model to study the effect of different parameters, such as combustor size, fuel property, fuel-air equivalence ratio and unburned mixture temper-

1. *School of Mechanical Engineering, Sharif University of Technology, P.O. Box 11155-9567, Tehran, Iran.*
*. *Corresponding author. E-mail: mssaidi@sharif.edu*

Received 15 December 2009; received in revised form 29 August 2010; accepted 2 October 2010

ature on the heat loss ratio and heat recirculation ratio. They derived a series of heat transfer equations and relations to study different parameters, and used three different combustible mixtures (H_2-air, CH_4-air and C_3H_8-air). They concluded that hydrogen is preferable to methane and propane due to higher flame temperature and thinner flame thickness. Lee and Kwon [10] proposed a heat loss model based on a simple theoretical analysis to study heat transfer and quenching in a micro combustion vessel. Li et al. [7] numerically simulated combustion at micro scale for two different diameters (2 mm and 6 mm), and studied the effect of diameter on the velocity, temperature and species mass fraction profiles; they mentioned that the combustion in micro scales has a 2-D nature. Leach et al. [11] have presented a simple analytical model for investigation of micro combustion and compared the results with a 1-D numerical model. Even though the main trend of the two models is the same, some have quantitative differences. Also they studied the effect of the temperature jump boundary condition (using Nusselt number as a function of Knudsen number) and stated that this effect can be neglected. They captured the reaction zone broadening phenomena for combustion in micro scales. Moreover, some other 2-D numerical simulations were conducted by researchers, but in almost all of them Fluent software was used to perform the simulations [12-14].

In the present work, a 2-D numerical method is used to investigate different parameters affecting combustion in micro scales. A home-made 2-D transient code is developed to do simulations. A H_2-air mixture with 9 species and 19 reactions is used (this parameter seems to be very important in micro scales combustion). In addition, heat transfer between surrounding and combustor walls is considered. Temperature and species mass fraction profiles for different heat transfer coefficients, micro combustor heights and inlet velocities are plotted at a steady state condition. Furthermore, the effect of applying slip flow and thermal creep boundary conditions is studied. The results of the present paper can be used to locate the flame zone in micro-scales. For different applications, the effect of various parameters can be compared, and only highly effective parameters lead to optimize the thermal behavior of a micro combustor.

COMPUTATIONAL DOMAIN, FORMULATION AND SOLUTION METHOD

Computational Domain and Boundary Conditions

In the present study, a cylindrical reactor is used, as shown schematically in Figure 1. The heat transfer to upstream by solid wall conduction is neglected, thus, the solid wall is not modeled in the present work.

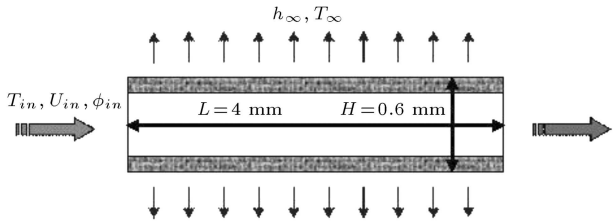

Figure 1. Schematic of micro combustor used in this work.

In this paper, the inlet temperature, velocity and equivalence ratio are assumed to be known. The heat transfer through the wall can be expressed as Equation 1:

$$q'' = h_\infty (T_w - T_\infty). \tag{1}$$

In the above equation, a fixed effective heat transfer coefficient (h_∞) is assumed for the wall heat loss.

The outlet boundary condition is somewhat complicated. Because wall heat loss is assumed, the flow does not reach a fully developed state. To overcome this problem, the length of the computational domain is spread to 6mm virtually, but wall heat loss for the latter 2 mm is supposed to be zero.

2-D Model Equations and Solution Method

In the present work, the characteristic length of the combustion chamber is sufficiently larger than the mean free path of the reacting flow gases. Thus, the continuum equations are reasonable. The transient 2-D model consists of continuity, momentums, energy transport and species mass transport equations that form an Advection-Diffusion-Reaction (ADR) system of equations. The gas radiation is neglected and the wall of the combustor is assumed to be inert (no absorption or desorption of species). Thus, energy and species mass balance equations are as follows:

$$\rho C_p \frac{dT}{dt} + \left(\rho C_p \vec{V} - \sum_{k=1}^{K} \rho C_{p,k} D \nabla Y_k \right) \cdot \nabla T = \nabla \cdot (\lambda \nabla T) - \sum_{k=1}^{K} h_k \dot{w}_k, \tag{2}$$

$$\rho \frac{dY_k}{dt} + \nabla \cdot \left(\rho \vec{V} Y_k \right) = \nabla \cdot (\rho D \nabla Y_k) + \dot{w}_k W. \tag{3}$$

In the present work, the flow is laminar and the reactants and products species are assumed to be ideal gases. Therefore, the density is obtained from the following equation:

$$\frac{1}{\rho} = \frac{1}{P} R_u T \sum_{k=1}^{K} \frac{Y_k}{W_k}. \tag{4}$$

The momentum equations are general Navier-Stokes equations and are not mentioned here. In the above equations, the energy equation, species mass transport equations and reaction rates are coupled to each other. T, Y_k and $\dot{w}_k$ are related to each other stiffly, which causes some difficulty in solving the above system of equations with conventional CFD algorithms. The dependency of density, heat capacity and velocity on the temperature and species mass fraction must be added to the above difficulty. In addition, because of using a multi-step chemistry mechanism with reaction rates of a very different order, the reaction rate calculation results in a stiff system of ODEs. Calculation of the reaction rate is explained in detail in the next section.

To solve these equations simultaneously, there are some algorithms, such as Operator Splitting (OS), Method Of Line (MOL), Semi-Implicit Spectral Differed Correction Method (SISDC) and Multi-Implicit Spectral Differed Correction Method (MISDC), which may be used. In the present study, the OS method is used. The idea behind this method is that a system is divided into subsystems that can be integrated in time [15]. The splitting technique has two main schemes:

1. First order scheme (linear),
2. Second or higher order scheme (non-linear).

Equations 2 and 3 are non-linear. Thus, the Strang Splitting method, which is suitable for a nonlinear stiff system of PDEs, is implemented. This method converts the nonlinear stiff systems of PDEs into two non-stiff systems of PDEs and two stiff systems of ODEs. The latter is solved using the VODE method (Variable-coefficient Ordinary Differential Equation), which is efficient and convenient [16]. The solution procedure is as follows:

- **Step 1.** Advection-Diffusion (A-D-1): In this step, energy and mass balance equations, excluding the reaction terms, are solved for the first half of the time-step:

$$\rho C_p \frac{dT^*}{dt} + \left(\rho C_p \vec{V} - \sum_{k=1}^{K} \rho C_{p,k} D \nabla Y_k \right) \cdot \nabla T^* = \nabla \cdot (\lambda \nabla T^*), \tag{5}$$

$$\rho \frac{dY_k^*}{dt} + \nabla \cdot \left(\rho \vec{V} Y_k^* \right) = \nabla \cdot (\rho D \nabla Y_k^*), \tag{6}$$

where $t_n < t < t_{n+\frac{1}{2}}$ and initial conditions are as below:

$$T^*(t_n) = T^n, \qquad Y_k^*(t_n) = Y_k^n. \tag{7}$$

- **Step 2.** Reaction (R): In this step, only the reaction term in the whole time-step is considered. Thus, the equations reduce to the following:

$$\rho C_p \frac{dT^{**}}{dt} = -\sum_{k=1}^{K} h_k \dot{w}_k, \tag{8}$$

$$\rho \frac{dY_k^{**}}{dt} = \dot{w}_k W, \tag{9}$$

where $t_n < t < t_{n+1}$ and initial conditions are as below:

$$T^{**}(t_n) = T^* \left(t_{n+\frac{1}{2}} \right), \qquad Y_k^{**}(t_n) = Y_k^* \left(t_{n+\frac{1}{2}} \right). \tag{10}$$

- **Step 3.** Advection-Diffusion (A-D-2): This step is the same as Step 1, but the flow field is solved for the 2nd half of the time-step:

$$\rho C_p \frac{dT^{***}}{dt} + \left(\rho C_p \vec{V} - \sum_{k=1}^{K} \rho C_{p,k} D \nabla Y_k \right) \cdot \nabla T^{***} = \nabla \cdot (\lambda \nabla T^{***}), \tag{11}$$

$$\rho \frac{dY_k^{***}}{dt} + \nabla \cdot (\rho \vec{V} Y_k^{***}) = \nabla \cdot (\rho D \nabla Y_k^{***}), \tag{12}$$

where $t_{n+\frac{1}{2}} < t < t_{n+1}$ and initial conditions are as follows:

$$T^{***} \left(t_{n+\frac{1}{2}} \right) = T^{**}(t_n), \qquad Y_k^{***} \left(t_{n+\frac{1}{2}} \right) = Y_k^{**}(t_n). \tag{13}$$

After all three steps are done for one time step, the new results are set as the initial conditions of the next time-step:

$$T^{n+1} = T^{***}(t_{n+1}), \qquad Y_k^{n+1} = Y_k^{***}(t_{n+1}). \tag{14}$$

The above procedure is repeated iteratively to reach the steady state condition. The finite volume method is used to discretize the continuity, momentum and advection-diffusion equations. Also, a hybrid differencing scheme and SIMPLEC algorithm is applied in the numerical code to do the pressure-velocity coupling and solve the discretized equations. In other words, the CFD code combines 3 main parts. First, the continuity, momentum and advection-diffusion equations are solved numerically using a conventional CFD method (SIMPLEC algorithm and hybrid differencing scheme in this work) in the first half of a time-step. Then, the

combustion calculations are done in the whole time-step. The VODE method is used in this part and new temperature and species mass fractions are obtained. The third part is similar to the first, but is done for the second half of a time-step and by means of the second part results as the initial values. The next time-step calculation is started afterwards.

Combustion Modeling

In this research, a multi-step and general reaction mechanism is considered:

$$\sum_{k=1}^{K} \nu'_{ki}\chi_k \Leftrightarrow \sum_{k=1}^{K} \nu''_{ki}\chi_k, \qquad (i = 1, 2, \cdots I). \tag{15}$$

The rate of production of each species is calculated from the following equation:

$$\dot{w}_k = \sum_{i=1}^{I} \nu_{ki} q_i, \qquad (k = 1, \cdots, K), \tag{16}$$

where the right hand side terms are as below:

$$\nu_{ki} = \nu'_{ki} - \nu''_{ki}, \tag{17}$$

$$q_i = \left(\sum_{k=1}^{K} a_{ki}[X_k]\right)\left(k_{fi}\prod_{k=1}^{K}[X_k]^{\nu'_{ki}} - k_{ri}\prod_{k=1}^{K}[X_k]^{\nu''_{ki}}\right). \tag{18}$$

The forward reaction rate constants can be calculated from the Arrhenius equation:

$$k_{fi} = A_i T^{\beta_i} \exp\left(\frac{-E_i}{RT}\right). \tag{19}$$

The reverse reaction rate constants are obtained from the following equations:

$$k_{ri} = \frac{k_{fi}}{k_{Ci}}, \tag{20}$$

$$k_{Ci} = k_{Pi}\left(\frac{P_{atm}}{RT}\right)^{\sum_{k=1}^{K}\nu_{ki}}, \tag{21}$$

$$k_{Pi} = \exp\left[\frac{\Delta S_i^\circ}{R} - \frac{\Delta H_i^\circ}{RT}\right], \tag{22}$$

$$\frac{\Delta S_i^\circ}{R} = \sum_{k=1}^{K} \nu_{ki}\frac{S_k^\circ}{R}, \tag{23}$$

$$\frac{\Delta H_i^\circ}{RT} = \sum_{k=1}^{K} \nu_{ki}\frac{H_k^\circ}{RT}, \tag{24}$$

$$\frac{S_k^\circ}{R} = a_{1k}\ln T_k + a_{2k}T_k + \frac{a_{3k}}{2}T_k^2 + \frac{a_{4k}}{3}T_k^3 + \frac{a_{5k}}{4}T_k^4 + a_{7k}, \tag{25}$$

$$\frac{H_k^\circ}{RT_k} = a_{1k} + \frac{a_{2k}}{2}T_k + \frac{a_{3k}}{3}T_k^2 + \frac{a_{4k}}{4}T_k^3 + \frac{a_{5k}}{5}T_k^4 + \frac{a_{6k}}{T_k}. \tag{26}$$

The above seven constants for species are obtained for two temperature ranges by the polynomial curve fitting of available data. The above relations form a stiff system of equations, which is solved using the VODE method.

Slip Flow and Thermal Creep Boundary Condition

Regarding the micro-scale nature of the present study, the velocity slip boundary condition must be modeled. In addition, the axial temperature gradient is significant in micro combustions, thus the thermal creep boundary condition is considered. This revised boundary condition can be expressed as follows [17]:

$$u_s - u_w = \frac{2-\sigma_v}{\sigma_v}L_{mfp}\left(\frac{\partial u}{\partial n}\right)_s + \frac{3}{4}\frac{\mu}{\rho T}\left(\frac{\partial T}{\partial s}\right)_s. \tag{27}$$

In the above equation, the wall velocity (u_w) is zero, and σ_v is the tangential momentum accommodation coefficient that has been assumed to be unity [17]. Usually, the Knudsen number (Kn) is used instead of the mean free path (L_{mfp}). These two parameters are related to each other by the following equation:

$$L_{mfp} = \mathrm{Kn} \times H,$$

where H is the micro combustor height.

Thermophysical Properties

The thermal diffusivity and conductivity of the gas mixture, as used by Kaisare and Vlachos, are assumed to be constant [8]. These values are considered to be 10^{-4} m^2/s and 0.1 W/mK, respectively (based on Nitrogen at 1500 K).

NUMERICAL RESULTS AND DISCUSSION

Two-Dimensional Numerical Results for Adiabatic Condition

In the first step, the contours of the temperature and [OH] mass fraction are shown in Figures 2 and 3.

These results show that the [OH] mass fraction has a significant effect on the burning of the H_2-Air mixture, and its maximum gradient region can be considered as a sign of the flame position. The following results show that for the adiabatic condition, the flame front is approximately from $x = 0.4$ mm to

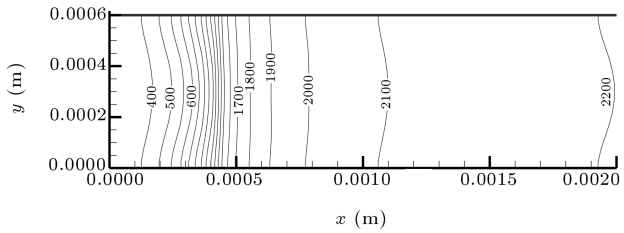

Figure 2. Temperature (K) contour for adiabatic condition.

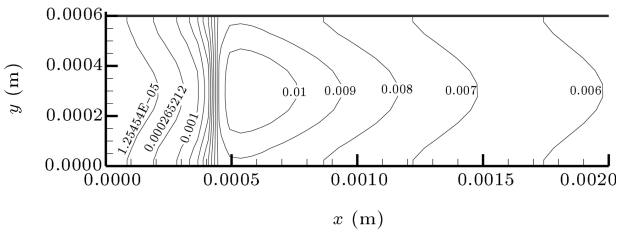

Figure 3. [OH] mass fraction contour for adiabatic condition.

$x = 0.6$ mm, where the temperature and the [OH] mass fraction change sharply. Thus, in the following charts, both the center line profile and the cross sectional profile of different parameters are shown at $x = 0.5$ mm. In addition, the results demonstrate that there is no flat part in the [OH] mass fraction. Consequently, the combustion in micro scales is two-dimensional in nature. This is in good agreement with the scale analysis done by Li et al. [7]. Their results show that flame flow in micro scale combustion is 2-D in nature, although the macro scale combustion could be treated as one-dimensional.

Effect of Thermal Creep and Slip Flow Boundary Conditions

To study the effect of a revised boundary condition on the temperature and species mass fraction profiles, slip velocity and thermal creep are considered in the code developed by using Equation 27. In this case, the parameters are:

$$h_\infty = 10 \text{ W/m}^2\text{.K}, \qquad u_{in} = 40 \text{ cm/s}, \qquad \phi = 1.0.$$

In Figures 4 and 5, the temperature and [OH] mass fraction profiles in the center line of the micro combustor for no slip and revised boundary conditions are compared.

The above results show that under investigated scales, applying slip flow and thermal creep boundary conditions has no significant effect on the flow and reaction characteristics at the center line of the micro combustor. To study this in more detail, the temperature profile at $x = 0.5$ mm is shown in Figure 6.

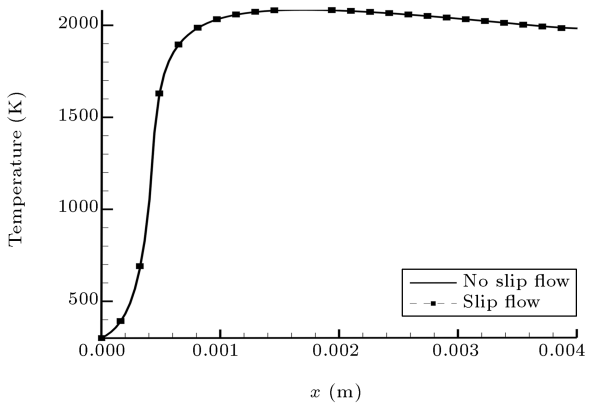

Figure 4. Center line temperature profile comparison for no slip and revised boundary conditions.

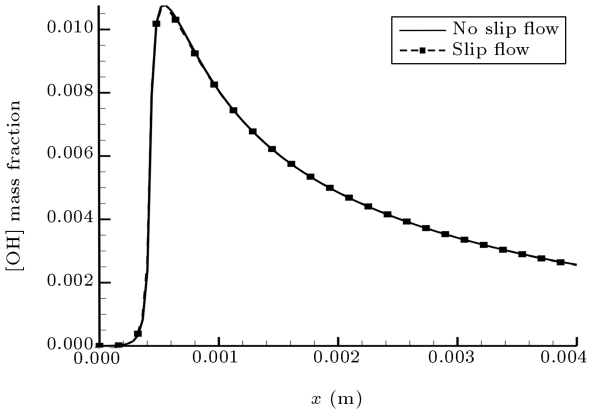

Figure 5. Center line [OH] mass fraction profile comparison for no slip and revised boundary conditions.

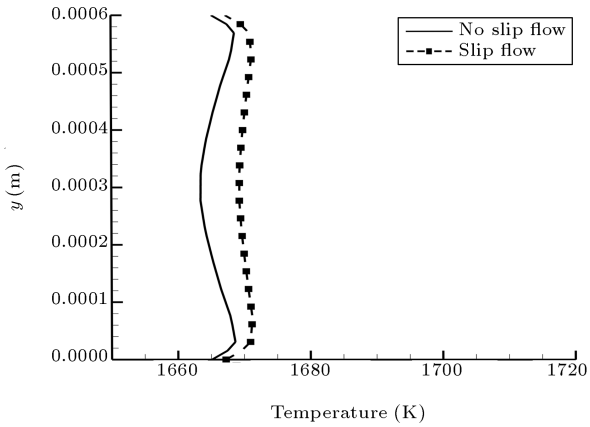

Figure 6. Cross section temperature profile comparison for no slip and revised boundary conditions at $x = 0.5$ mm.

The results show that applying revised boundary conditions leads to about a 7 K (0.04%) temperature rise at the midpoint of the micro burner. Thus, as a result of the numerical investigation, the revised boundary condition is not of primary importance to the temperature and species mass fraction field in the simulated scales.

Effect of Convection Heat Transfer Coefficient

The effect of convection heat transfer coefficient on temperature, [OH] and [O_2] mass fraction profiles are investigated and the results are shown in Figures 7-9.

It is clear from the results that increasing the convection heat transfer coefficient increases the heat loss from the lateral wall of the micro combustor. Therefore, it reduces the maximum temperature of combustion. Consequently, the concentration of radicals at the outlet decreases. The effect of this parameter on the [OH] mass fraction profile is more pronounced than the [O_2] mass fraction profile.

The cross section temperature profile at $x = 0.5$ mm is shown in Figure 10. It shows that the trend of the temperature profile changes by increasing the convection heat transfer coefficient with the surroundings. For the adiabatic condition at the proposed coordinate, the temperature near the wall is greater than the center line temperature. However, by increasing the convection heat transfer coefficient with the surroundings, the wall temperature becomes

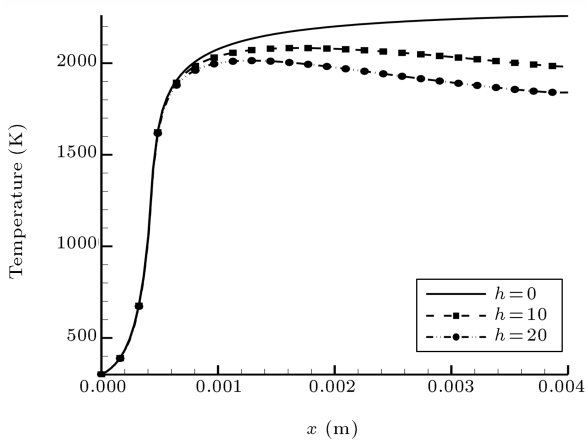

Figure 7. Center line temperature profile for different convection heat transfer coefficients.

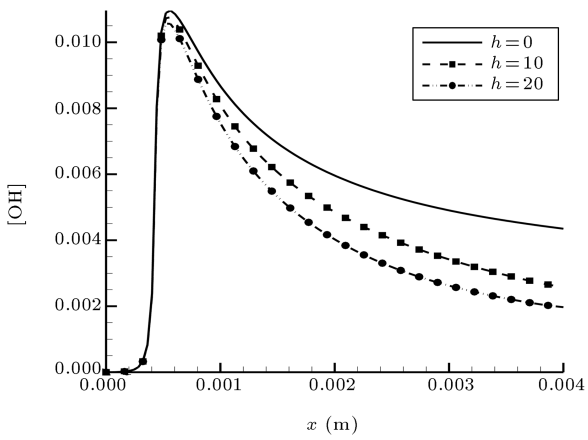

Figure 8. Center line [OH] mass fraction profile for different convection heat transfer coefficients.

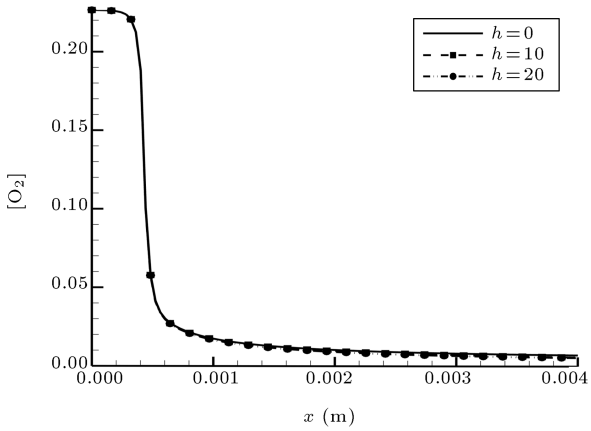

Figure 9. Center line O_2 mass fraction profile for different convection heat transfer coefficients.

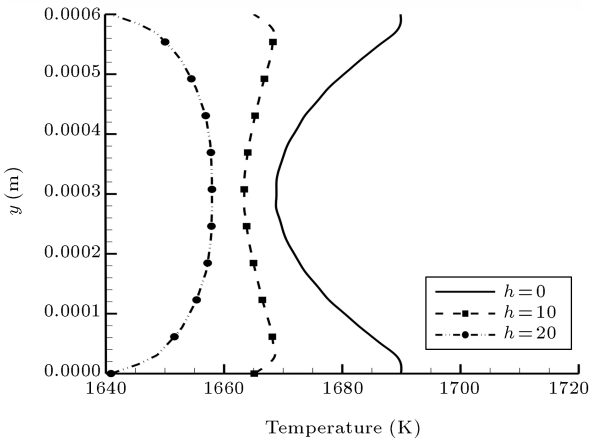

Figure 10. Cross section temperature profile comparison for different convection heat transfer coefficients at $x = 0.5$ mm.

less than the center line temperature at $x = 0.5$ mm. Moreover, in all vertical positions of the combustor, the temperature is reduced by increasing the lateral heat transfer coefficient. The two-dimensional nature of combustion at the micro scale is another result of Figure 10. This is because of the existence of curvature in the cross section temperature profiles.

Effect of Inlet Mixture Velocity

Another parameter that influences the combustion in micro scales is the inlet mixture velocity. This parameter affects both the heat generation rate and the maximum temperature position inside the micro combustor. For this purpose, three different inlet mixture velocities have been studied: 30 cm/s, 40 cm/s and 50 cm/s. The numerical results are illustrated in Figures 11 to 13.

These figures illustrate that decreasing the inlet mixture velocity leads to a reduction in temperature along the combustor and a decrease in the mass

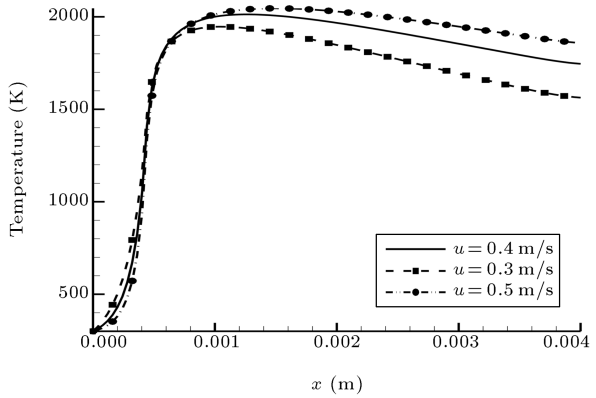

Figure 11. Center line temperature profile for different inlet mixture velocities.

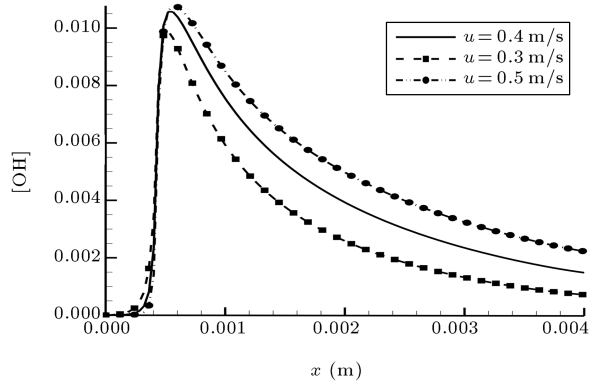

Figure 12. Center line [OH] mass fraction profile for different inlet mixture velocities.

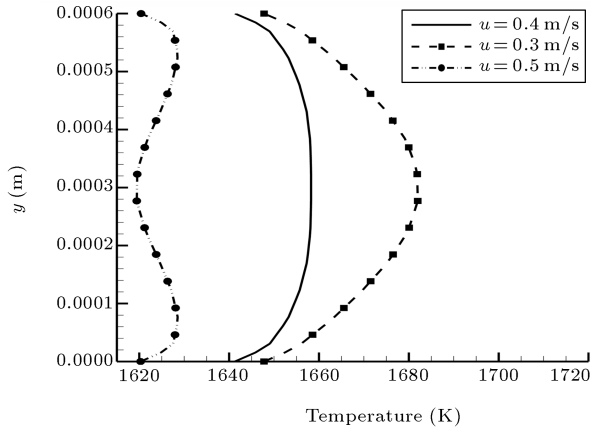

Figure 13. Cross section temperature profile comparison for different inlet mixture velocities at $x = 0.5$ mm.

fractions of the effective radicals. It must be mentioned that the temperature and mass fraction of effective radicals are proportional to each other. Also, the preceded figures show that the position of the maximum temperature or flame position is moved forward along the axis by increasing the inlet mixture velocity. By increasing the inlet velocity, the flame gets swept out of the combustor and the blowout phenomenon occurs. This phenomenon shows that there is a lower limit for the length of micro combustors, which must be considered in the design and manufacturing of such components. Figure 13 illustrates that in $x = 0.5$ mm, the flame temperature is decreased by increasing the inlet mixture velocity. This shows that the flame is not formed for an inlet velocity of 0.5 m/s at the investigated horizontal position.

Effect of Micro Combustor Height

To study the effect of micro combustor height on the temperature and mass fraction profiles, two different heights are simulated: 0.6 mm and 0.4 mm. The numerical results are shown in Figures 14-17. It should be noted that because the heights are different in this case, normalized instead of actual height is used.

The results show that in micro scales, the height of the combustor has a significant effect on the temperature profile. Decreasing the micro combustor height increases the area-to-volume ratio and, consequently,

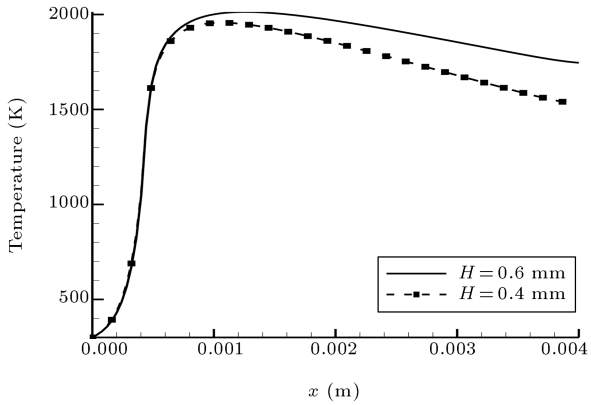

Figure 14. Center line temperature profile for different micro combustor heights.

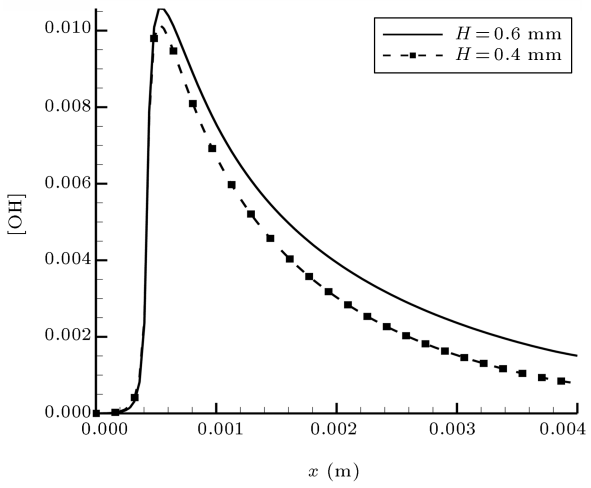

Figure 15. Center line [OH] mass fraction profile for different micro combustor heights.

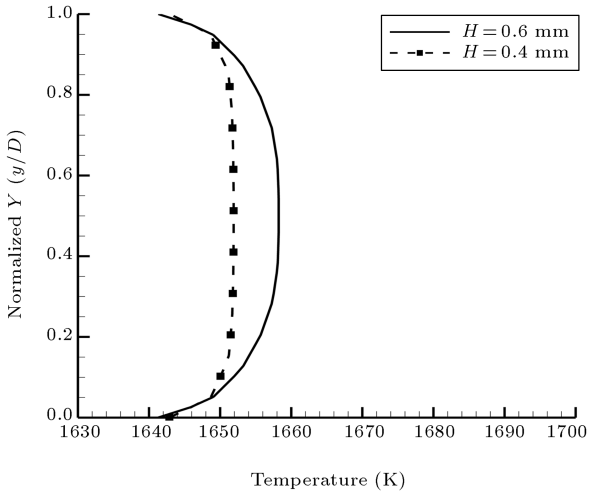

Figure 16. Cross section temperature profile comparison for different micro combustor heights at $x = 0.5$ mm.

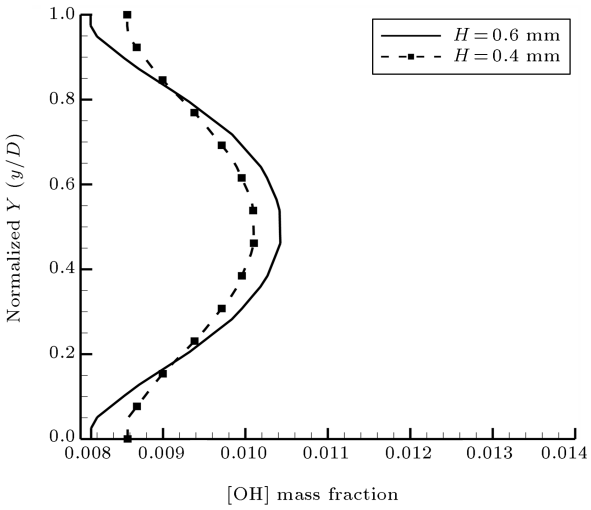

Figure 17. Cross section [OH] mass fraction profile comparison for different micro combustor heights at $x = 0.5$ mm.

increases the heat loss from the combustor. This effect is usually neglected at macro scale. It seems that by decreasing the height more and more, the flame may be quenched. In addition, this reduction decreases the effective radicals' concentration along the micro combustor.

Figures 16 and 17 show that the form of the cross section temperature and [OH] mass fraction profiles is the same for the two different heights. Although the temperature and [OH] mass fraction at the center of the combustor is proportional to the height, near the wall it is the other way around. It should be noted that the average temperature and [OH] mass fraction at $x = 0.5$ mm is higher for $H = 6$ mm. Also these figures show that these two profiles have no flat part. Thus, flame flow at the micro scale could be treated as two-dimensional.

CONCLUSION

In the present work, a 2-D numerical approach has been adopted to investigate the effect of various parameters, such as convection heat transfer coefficient, inlet mixture velocity and micro combustor height, on the combustion and heat transfer rates in a cylindrical micro scale combustor. Since one-step chemistry cannot represent real combustion, a multi-step chemistry mechanism for a H_2-air mixture is implemented. Moreover, a lateral convection heat transfer with a surrounding is considered. Also, the effects of slip flow and thermal creep boundary conditions have been investigated in the present study.

The numerical simulations indicate that under the investigated scales, the slip flow and thermal creep boundary conditions have no significant effect on the temperature and species mass fraction profiles. In addition, the numerical results show that in contrast to the macro scales, heat transfer with a surrounding thorough the combustor walls has a significant effect on the combustion and heat transfer characteristics at micro scale. This is because of higher area-to-volume ratio, and consequently, extra heat loss in the micro scales.

The numerical simulations illustrate that the flame zone is a very thin region, which is near the micro combustor inlet under the investigated lengths and inlet mixture velocities. The cross sectional changes of temperature and [OH] mass fraction confirm the two-dimensional nature of combustion at micro scale. In addition, increasing the convection heat transfer coefficient and decreasing the combustor height as two major parameters in micro scale devices decreases the temperature and radical species concentrations in the flame zone. Moreover, increasing the inlet mixture velocity and micro combustor height increases the temperature, but increasing the inlet velocity forwards the flame position at micro scale. Therefore, the length of the micro combustor should be checked for prevention of flame sweep up.

NOMENCLATURE

A	pre-exponential factor
a	third body, species thermal constant
C	heat capacity
D	diffusion coefficient
E	activation energy
H	enthalpy, height
h	heat transfer coefficient, specific enthalpy
k	rate constant
Kn	Knudsen number

L	length
n	time step, normal direction
q	rate of progress
q''	wall heat loss
P	pressure
R	gas constant
S	entropy
T	temperature
t	time
u	ith velocity component
$\vec{V}$	velocity vector
W	molar weight
X	mole fraction
x	space coordinate in the ith direction
$[X]$	mole concentration
Y	mass fraction
Y	space coordinate in the jth direction

Greek Symbols

β	temperature exponent
ϕ	equivalence ratio
λ	thermal conductivity
μ	viscosity
ρ	density
σ	accommodation coefficient
ν	stoichiometric coefficient
$\dot{\omega}$	production rate
χ	species symbol

Subscripts and Superscripts

atm	atmosphere
c	concentration
f	forward
i	reaction
I	number of reactions
in	inlet
j	grid
K	number of species
k	species
mfp	mean free path
p	pressure
r	reverse
s	tangential
u	universal
v	velocity
w	wall
$'$	forward stoichiometric coefficient
$''$	reverse stoichiometric coefficient
$^\circ$	standard
∞	surrounding

REFERENCES

1. Waitz, I.A., Gauba, G. and Yang, S.T. "Combustors for micro-gas turbine engines", *Journal of Fluids Engineering*, **120**, pp. 109-117 (1998).
2. Jin, P., Gao, Y.L., Liu, N., Tan, J.B. and Jiang, K. "Design and fabrication of alumina micro reciprocating engine", *Journal of Physics: Conference Series*, **48**, pp. 1471-130 (2006).
3. Lee, K.H. and Kwon, O.C. "Studies on a heat-recirculating microemitter for a micro thermophotovoltaic system", *Combustion and Flame*, **153**, pp. 161-172 (2008).
4. Yang, W.M., Chou, S.K., Shu, C., Xue, H., Li, Z.W., Li, D.T. and Pan, J.F. "Microscale combustion research for application to micro thermophotovoltaic systems", *Energy Conversion and Management*, **44**, pp. 2625-2634 (2003).
5. Vahabi, M. and Akhbari, M.H. "Three-dimensional simulation and optimization of an isothermal PROX microreactor for fuel cell applications", *International Journal of Hydrogen Energy*, **34**, pp. 1531-1541 (2009).
6. Fernandez-Pello, A.C. "Micro-power generation using combustion: Issues and approaches", *Twenty-Ninth International Symposium on Combustion*, Sapporo, Japan (2002).
7. Li, Z.W., Chou, S.K., Shu, C., Xue, H. and Yang, W.M. "Characteristics of premixed flame in micro-combustors with different diameters", *Applied Thermal Engineering*, **25**, pp. 271-281 (2005).
8. Kaisare, N.S. and Vlachos, D.G. "Optimal reactor dimensions for homogenous combustion in small channels", *Catalysis Today*, **120**, pp. 96-106 (2007).
9. Li, J., Chou, S.K., Li, Z. and Yang, W. "Development of 1-D model for the analysis of heat transport in cylindrical micro combustors", *Applied Thermal Engineering*, **29**, pp. 1854-1863 (2009).
10. Lee, D.H. and Kwon, S. "Heat transfer and quenching analysis of combustion in a micro combustion vessel", *Journal of Micromechanics and Microengineering*, **12**, pp. 670-676 (2002).
11. Leach, T.T., Cadou, C.P. and Jackson, G.S. "Effect of structural conduction and heat loss on combustion in micro-channels", *Combustion Theory and Modeling*, **10**(1), pp. 85-103 (2006).
12. Hua, J., Wu, M. and Kumar, K. "Numerical simulation of the combustion of hydrogen-air mixture in micro-scaled chambers. Part I: Fundamental study", *Chemical Engineering Science*, **60**, pp. 3497-3506 (2005).
13. Norton D.G. and Vlachos D.G. "A CFD study of propane/air microflame stability", *Combustion and Flame*, **138**, pp. 97-107 (2004).

14. Norton, D.G. and Vlachos, D.G. "Combustion characteristics and flame stability at the microscale: a CFD study of premixed methane/air mixtures", *Chemical Engineering Science*, **58**, pp. 4871-4882 (2003).

15. Sportisse, B. "An analysis of operating splitting techniques in the stiff case", *Journal of Computational Physics*, **161**, pp. 140-168 (2000).

16. Brown, P.N., Byrne, G.D. and Hindmarsh, A.C. "VODE, a variable-coefficient ODE solver", *SIAM Journal of Scientific and Statistical Computing*, **10**(5), pp. 1038-1051 (1989).

17. Kandlikar, S., Garimella, S., Li, D., Colin, S. and King, M.R., *Heat Transfer and Fluid Flow in Minichannels and Microchannels*, Elsevier Inc. (2006).

BIOGRAPHIES

Abolfazl Irani Rahaghi is a M.S. degree student in the Mechanical Engineering School at Sharif University of Technology, Tehran, Iran. He has been working with Professors M.H. Saidi and M.S. Saidi since September 2007 in the area of Combustion Modeling and Simulation. This work specifically involves the Modeling of a Two-Stage Porous Media Burner and 1-D and 2-D Numerical Simulation of a Micro Combustor.

Mohammad Said Saidi is the professor of mechanical engineering at Sharif University of Technology. His research interests are: Modeling and Numerical Analysis of Transport and Deposition of Aerosol Particles, Modeling and Numerical Analysis of Biofluids, Modeling and Numerical Analysis of Thermal-Hydraulics of Porous Media and Microchannels.

Mohammad Hassan Saidi is Professor and Chairman of the School of Mechanical Engineering at Sharif University of Technology, Tehran, Iran. His current research interests include: Heat Transfer Enhancement in Boiling and Condensation, Combustion Modeling and Simulation, Modeling of Pulse Refrigeration, Vortex Tube Refrigerators, Indoor Air Quality and Clean Room Technology and Energy Efficiency in Home Appliances and Desiccant Cooling Systems.

Mohammad Behshad Shafii was a Ph.D. student in Mechanical Engineering at Michigan State University, USA, from 2000-2005 and is currently an Assistant Professor in the Mechanical Engineering School at Sharif University of Technology, Tehran, Iran. His research interests include: Fluid Diagnostic Techniques (MTV, PIV and LIF), Heat Transfer, Phase Change, Micro-pumps and Heat Pipes.